Molecular Psychiatry

Deficiency of calcium/calmodulin-dependent serine protein kinase (CASK) disrupts the excitatory-inhibitory balance of synapses by down-regulating GluN2B.

Running title: CASK deficiency affects synaptic balance via GluN2B

Takuma Mori[1,7], Enas A. Kasem[1,2,7], Emi Suzuki-Kouyama[1], Xueshan Cao[1], Xue Li[1], Taiga Kurihara[1], Takeshi Uemura[1,3,5], Toru Yanagawa[4] & Katsuhiko Tabuchi[1,3,6*]

[1]Department of Molecular and Cellular Physiology, Institute of Medicine, Academic Assembly, Shinshu University, Nagano 390-8621, Japan

[2]Department of Zoology, Faculty of Science, Kafr Elsheikh University, Kafr Elsheihk, 33511, Egypt

[3]Institute for Biomedical Sciences, Interdisciplinary Cluster for Cutting Edge Research, Shinshu University, Nagano 390-8621, Japan

[4]Department of Oral and Maxillofacial Surgery, Faculty of Medicine, University of Tsukuba, Ibaraki 305-8575, Japan

[5]CREST, JST, Saitama 332-0012, Japan

[6]PRESTO, JST, Saitama 332-0012, Japan

[7]These authors contributed equally to this work.

Abstract: 163 words.

Words: 3,500 words.

Figures: 5

Supplemental Figures: 10

Supplemental Table: 1

Abstract

Calcium/calmodulin-dependent serine protein kinase (CASK) is a membrane-associated guanylate kinase protein (MAGUK) that is associated with neurodevelopmental disorders. CASK is thought to have both pre- and postsynaptic functions, but the mechanism and consequences of its functions in the brain have yet to be elucidated, because homozygous CASK-KO mice die before brain maturation. Taking advantage of the X-chromosome inactivation (XCI) mechanism, here we examined the synaptic functions of CASK-KO neurons in acute brain slices of heterozygous CASK-KO female mice. We also analyzed CASK knock-down (KD) neurons in acute brain slices generated by in utero electroporation. Both CASK-KO and CASK-KD neurons showed a disruption of the excitatory and inhibitory (E/I) balance. We further found that the expression level of the NMDA receptor subunit GluN2B was decreased in CASK-KD neurons and that overexpressing GluN2B rescued the disrupted E/I balance in CASK-KD neurons. These results suggest that the down-regulation of GluN2B may be involved in the mechanism of the disruption of synaptic E/I balance in CASK-deficient neurons.

37 **Introduction**

38 Calcium/calmodulin-dependent serine protein kinase (CASK) is a membrane-associated guanylate
39 kinase protein (MAGUK) that consists of N-terminal calcium/calmodulin kinase-like (CAM), LIN,
40 PDZ, SH3, and C-terminal guanylate kinase (GK) domains[1-3]. CASK interacts with other synaptic
41 proteins involved in cell adhesion, cytoskeletal organization, signal transduction, and/or gene
42 transcription[4-12], and is thought to have both pre- and postsynaptic functions. As a postsynaptic role,
43 CASK is translocated to the nucleus and functions as a co-activator of transcription regulatory factor
44 TBR1, a T-box transcription factor, through binding at its GK domain[13]. The cooperation of CASK and
45 TBR1 facilitates the transcription of T-element-containing genes, such as Reelin and the NMDA
46 receptor subunit GluN2B[13-15].

47 Genomic variants of CASK have been linked to neurodevelopmental disorders[16], including mental
48 retardation with or without nystagmus[17, 18], Otahara syndrome[19], infantile spasms[20, 21], mental retardation
49 and microcephaly with pontine and cerebellar hypoplasia (MICPCH)[22, 23], and FG syndrome 4[24, 25].
50 Variants that disrupt the entire CASK protein, such as deletions or stop mutations located in N-terminal
51 regions, have been identified only in females[26]. CASK mutations may affect males more severely[27]
52 because the human CASK gene is located on the X-chromosome (mapped to Xp11.4)[28, 29]. The
53 complete loss of CASK is probably lethal, as observed in knockout mice[30]. Genes on the
54 X-chromosome are subjected to X-chromosome inactivation (XCI) in female humans[31] and mice[32].
55 During early embryogenesis, one of the two alleles of the X-chromosome is randomly selected and
56 inactivated by non-coding RNA called an X-inactive specific transcript. The inactivated and activated
57 pair of X-chromosomes is transmitted to daughter cells after every cell division, resulting in a random
58 mixture of cells with two different X genotypes throughout the body. Thus, both CASK-intact and
59 CASK-deficient cells are likely to be distributed in a mosaic pattern in the brain of affected females. The

60 mosaicism of CASK mutant neurons affects normal brain networks and may be responsible for the
61 pathogenesis of neurological disorders.
62 The synaptic functions of CASK-knockout (CASK-KO) mice were previously analyzed in dissociated
63 cortical cultured neurons[30]. CASK-KO disrupts the balance between excitatory and inhibitory (E/I)
64 synaptic functions, as indicated by an increase in the frequency of miniature excitatory postsynaptic
65 currents (mEPSCs) and a decrease in the frequency of miniature inhibitory postsynaptic currents
66 (mIPSCs).
67 Despite accumulating knowledge about CASK at the protein and cellular levels, its functions in the
68 brain remain elusive. Here we examined the effect of CASK on synaptic function in acute brain slices,
69 taking advantage of XCI and in utero electroporation. In patch-clamp electrophysiological analyses,
70 both CASK-KO and CASK-KD pyramidal neurons in the forebrain replicated the disrupted E/I balance
71 phenotype observed in cultured KO neurons. Since CASK-deficient neurons are distributed in a mosaic
72 pattern in these tissues, we concluded that this effect was caused by a postsynaptic CASK deficiency.
73 Rescue experiments in CASK-KD neurons showed that this disrupted E/I balance was due to the
74 down-regulation of GluN2B transcription, which is normally promoted by the cooperation of TBR1 and
75 CASK.
76
77 **Materials and Methods**
78 All animal procedures were approved by the Animal Care and the Use Committee of Shinshu
79 University School of Medicine. Detailed procedures are described in the Supplementary Information.
80
81 **Animals.** CASK-KO mice were obtained by crossing mice carrying floxed CASK
82 (B6;129-Cask^{tm1Sud}/J, JAX Stock #006382)[30] and ZP3-Cre (C57BL/6-Tg(Zp3-cre)93Knw/J[33], JAX
83 Stock #003651).

84

85 **Plasmid construction.** shRNA constructs (see Supplementary Information for target sequences) were
86 cloned into an L309 backbone vector[34]. The CASK, GluN2B, and tdTomato genes in eukaryotic expression
87 vectors were driven by a CAG promoter.

88

89 ***In utero* electroporation.** *In utero* electroporation was performed essentially as described previously[35,
90 36]. Briefly, pregnant ICR mice at E15.5 were anesthetized, and the uterine horns were exposed.
91 Approximately 1 μl of DNA solution was injected into the lateral ventricles of embryos. The embryos
92 were subjected to five square electric pulses (35 V, 50 ms, 1 Hz) using an electroporator (CUY21E;
93 NEPA Gene). The brains with abnormal morphology were excluded from the experiments.

94

95 **Electrophysiology.** Slice recording was performed essentially as described previously[35]. P14-P18
96 mouse brains were cut into 350-μm-thick coronal sections. In the current clamp experiments, pyramidal
97 neurons were patched with a glass pipette containing potassium-based intra-cellular solution (ICS) or
98 cesium-based ICS. Miniature postsynaptic currents (mPSCs) were recorded in the presence of 1 μM
99 tetrodotoxin (Abcam). Membrane potential was held at -60 mV for mEPSCs and 0 mV for mIPSCs.
100 Evoked postsynaptic currents were triggered with a 0.1-ms current injection by a nichrome-wire
101 electrode placed 100-150 μm from the soma of recorded neurons.

102

103 **Single-cell RT-PCR.** Single-cell RT-PCR was performed as described previously with modifications[35].
104 After the RT reaction, single-cell cDNA was amplified by two rounds of semi-nested PCR with the
105 primers listed in Supplementary Table 1. The animals were genotyped before recording and recorded
106 cells were genotyped after the recording for blind experiments.

107

108 **Measurement of CASK and GluN2B mRNA levels in knock-down cultured neurons.** Quantitative
109 RT-PCR (qRT-PCR) was performed using the RNA isolated from cultured primary cortical neurons
110 infected with shRNA-expressing lentivirus. The cells were harvested and lysed, and the total RNA was
111 purified with Trizol reagent (Invitrogen). After cDNA synthesis, real-time PCR reactions (see
112 Supplementary Table 1 for primers) were run and analyzed on a StepOnePlus system (Thermo Fisher).
113
114 **Sample size and Statistical analysis.** Samples sizes were determined based on established
115 practice and on our previous experience in respective assays[30, 35, 37]. The number of
116 independent samples (e.g. neurons) is indicated on the graphs and the numbers of animals
117 indicated in the figure legends. All values represent the average of independent experiments ±
118 SEM. The variance among analyzed samples was similar. Statistical significance was determined by
119 Student's t-test (for two groups) or one-way ANOVA followed by Bonferroni's post-hoc test (for
120 multiple groups). Statistical analysis was performed with Prism 6.0 (Graphpad Software Inc.). Statistical
121 significance is indicated by asterisks (* $p < 0.05$, ** $p < 0.01$, *** $p < 0.001$).
122
123 **Results**
124 **Heterozygous CASK-KO mice exhibit a hypomorphic phenotype and a mosaic distribution of**
125 **CASK-deficient neurons in the brain due to XCI.**
126 To examine the physiological role of CASK, we studied the effect of CASK-KO in adult mouse brain.
127 As described previously[30], all CASK-KO mice ($CASK^{Y/-}$) died within 24 hours after birth. In contrast,
128 the survival and growth of heterozygous female KO mice ($CASK^{+/-}$) varied among individuals.
129 Approximately 75% of the $CASK^{+/-}$ mice were viable at P15 (Figure 1a), with 63.5%-102.9% of the
130 mean wild-type (WT) body weight (Figure 1b and c). The cerebellar cortex was smaller in the $CASK^{+/-}$
131 mice compared to WT (Supplementary Figure 1a), but its overall structure, including its laminar

132 arrangement, was normal (Figure 1d and Supplementary Figure 1b). We did not observe apparent
133 spontaneous seizures, but found a reduction of seizure threshold in CASK$^{+/-}$ mice by
134 pentylenetetrazol-injection (Supplementary Figure 1c and 1d).

135 We speculated that the variable survival and body weight of the CASK$^{+/-}$ mice was due to XCI. Thus,
136 we examined the CASK genotype in single neurons in acute brain slices of CASK$^{+/-}$ mice by single-cell
137 RT-PCR, using cytosol from pyramidal neurons extracted through patch pipettes[35] (Figure 1e and f). We
138 found that approximately half (46.6 %) of these neurons expressed CASK mRNA while half did not
139 (Figure 1g), suggesting that CASK was subjected to XCI. The same method was used hereafter to
140 determine the CASK genotype in neurons recorded by patch-clamp electrophysiology in CASK$^{+/-}$ mice.

141 CASK is known to affect the properties of ion channels, including calcium (e.g., Cav1.2)[38, 39], inward
142 rectifier potassium (Kir2)[40], and voltage-gated sodium (NaV 1.5)[41] channels. To investigate whether
143 CASK deletion affected the function of ion channels in neocortical pyramidal neurons, we examined the
144 membrane properties and excitability in CASK$^{+/-}$-KO neurons by whole-cell recording in the current
145 clamp mode (Figure 1h). In this experiment, we did not detect changes in any of the parameters we
146 tested, including the resting potential, threshold of action potential (AP), amplitude of AP, half-time
147 width of AP, input resistance, or input-output relationship between the injected current amount and spike
148 numbers (Figure 1i-n), suggesting that the CASK deletion did not affect the intrinsic excitability in
149 cortical pyramidal neurons.

150

151 **Postsynaptic CASK deficiency during development disrupts the E/I balance in synaptic**
152 **transmission in heterozygous CASK-KO mice.**

153 Next, to examine the effect of CASK deficiency on synaptic function, we studied the spontaneous
154 mPSCs in CASK$^{+/-}$ and WT mice. We recorded both the mEPSCs and mIPSCs from each pyramidal
155 neuron in layer 2/3 of the somatosensory cortical slices in CASK$^{+/+}$, CASK$^{Y/+}$, and CASK$^{+/-}$ mice. We

156 identified the genotypes of the postsynaptic neurons by single-cell RT-PCR after recording as described
157 above. We found that the frequency but not the amplitude of the mEPSCs was significantly increased in
158 the CASK$^{+/-}$-KO neurons in CASK$^{+/-}$ mice (Figure 2a-c). In contrast, the frequency but not the
159 amplitude of the mIPSCs was decreased in the CASK$^{+/-}$-KO neurons in CASK$^{+/-}$ mice (Figure 2d-f). A
160 scatter plot revealed that the distribution of the frequency of mEPSCs versus mIPSCs in CASK$^{+/-}$-KO
161 neurons was different from that in the other genotypes (Figure 2g). The E/I balance index in
162 CASK$^{+/-}$-KO neurons (0.615 ± 0.016) was significantly higher than that in the WT genotypes (CASK$^{+/+}$
163 $= 0.267 \pm 0.013$, CASK$^{Y/+}$ $= 0.262 \pm 0.015$, CASK$^{+/-}$-WT neurons $= 0.259 \pm 0.021$, $p < 0.001$, ANOVA,
164 Bonferroni's post-hoc test; Figure 2h). Similar phenotypes were also observed in the pyramidal neurons of
165 the CA1 region of the hippocampus (Supplementary Figure 2). In CASK$^{+/-}$ mice, approximately half of
166 the presynaptic inputs onto recording neurons should be CASK-positive and the other half
167 CASK-negative. The genotype-dependent phenotype of the recording neurons suggested that these
168 effects were caused by CASK deficiency in the postsynaptic neurons.
169 Next, to address whether the disrupted E/I balance phenotype in CASK$^{+/-}$-KO neurons was due to the
170 absence of CASK during neural development or after synapse formation, we knocked out CASK in the
171 adult cerebral cortex by AAV-mediated cre recombination. We injected AAV-GFP-Cre or AAV-GFP into
172 the somatosensory cortex of CASK floxed mice at P10-13 and analyzed mPSCs in acute brain slices at
173 P24-28 (Figure 2i). We recorded from the GFP-Cre-positive cells, in which CASK was knocked out by
174 cre recombination. The adult CASK-KO neurons exhibited unaltered mPSCs (Figure 2j and k),
175 suggesting that the disrupted E/I balance was caused by the CASK deficiency during neural
176 development.
177
178 **CASK deficiency impairs NMDA receptor-mediated synaptic function.**

179 Alterations in the frequency but not in the amplitude of mPSCs indicated that presynaptic functions
180 projecting to the CASK$^{+/-}$-KO neurons might have been impaired. To examine the release probability of
181 presynaptic inputs, we analyzed the paired-pulse ratio (PPR) of the excitatory and inhibitory
182 neurotransmission evoked by electrical stimulation. We found that the PPRs of both excitatory and
183 inhibitory inputs were unaltered in the CASK$^{+/-}$-KO neurons (Figure 2l), indicating that CASK
184 deficiency did not affect the release probability of synaptic inputs, but instead might have affected the
185 number of functional synapses. We further investigated the NMDA receptor function by measuring the
186 evoked NMDA currents recorded at a holding potential of +40 mV. We found that the NMDA/AMPA
187 ratio and NMDA decay time constant were decreased in the CASK$^{+/-}$-KO neurons (Figure 2m).
188
189 **Postsynaptic CASK KD disrupts the E/I balance of synaptic transmission and downregulates the**
190 **expression of GluN2B.**
191 To investigate the mechanism by which CASK regulates the E/I balance of synapses during neural
192 development, we knocked-down CASK specifically in a population of pyramidal neurons in layer 2/3
193 of the somatosensory cortex using *in utero* electroporation. The CASK mRNA level in the KD neurons
194 was decreased to 13.5% of that found in control virus-infected neurons (Supplementary Figure 3a). The
195 CASK-KD neurons showed normal migration in the six-layer cortical structure (Supplementary Figure
196 3b) and unaltered spine density (Supplementary Figure 4). CASK-KD also did not affect the membrane
197 properties or the intrinsic excitability of neurons (Supplementary Figure 5).
198 We next measured the mEPSCs and mIPSCs in the CASK-KD neurons. Consistent with the results of
199 CASK$^{+/-}$-KO neurons, the CASK-KD neurons had mEPSCs with an increased frequency but unaltered
200 amplitude (Figure 3a-c), and mIPSCs with a decreased frequency and unaltered amplitude (Figure 3d-f).
201 The scatter plot of the frequency of mEPSCs versus mIPSCs was different for the CASK-KD neurons
202 compared to controls (Figure 3g). The E/I balance index of the CASK-KD neurons (0.583 ± 0.022;

203 Figure 3h) was greater than that of controls (0.295 ± 0.022). Like CASK-KO, CASK-KD showed no
204 change in the either the excitatory or inhibitory PPRs (Supplementary Figure 6).
205 CASK contains CAM, LIN, PDZ, SH3, and GK domains. To investigate which domain of CASK is
206 responsible for the synaptic phenotype, we performed rescue experiments in which we co-expressed
207 deletion mutants of CASK lacking each domain in CASK-KD neurons (Supplementary Figure 7). The
208 co-expression of CASK lacking the CAM (ΔC), LIN (ΔL), PDZ (ΔP), or SH3 (ΔS) domain, as well as
209 CASK full-length (FL), restored the frequency of both the mEPSCs and mIPSCs to the control levels
210 (Figure 3a-f). However, CASK lacking the GK domain (ΔG) failed to rescue the altered frequencies of
211 mEPSCs/mIPSCs and the disrupted E/I balance (Figure 3a-h).
212 Consistent with the results in CASK-KO neurons, CASK-KD impaired the NMDA receptor function.
213 The NMDA/AMPA ratio and decay time constant were decreased in CASK-KD neurons (Figure 3i-l),
214 and these phenotypes were not rescued by co-expressing the CASK ΔG construct (Figure 3i-l). A
215 shortened decay time constant of the NMDA receptor-mediated current implies that the composition of
216 NMDA receptor subunits is altered[42]. We therefore examined the expression levels of GluN2A and
217 GluN2B in CASK-KD cultured neurons and found that the GluN2B expression was selectively
218 decreased (Figure 3m).
219 The GluN2B expression is known to be regulated by T-box transcription factor TBR1 bound to the
220 GK domain of CASK[15]. Indeed, we detected TBR1 immunoreactivity mostly in the layer 2/3 neurons
221 of P14 mice (Supplementary Figure 8). To examine whether the synaptic phenotype of CASK-deficient
222 neurons was related to the CASK/TBR1 interaction, we co-transfected them with CASK containing a
223 T704A mutation, which interferes with CASK's binding to TBR1, in the CASK-KD neurons and
224 analyzed mPSCs[43-45]. Like the CASK ΔG mutant, the CASK T704A mutant failed to rescue the
225 aberrant frequencies of mEPSCs and mIPSCs (Figure 3b,e).
226

227 **GluN2B-KD replicates the disrupted E/I balance of synaptic transmission.**

228 Next, we examined the effects of GluN2B deficiency on synapses using GluN2B-KD and compared
229 them to those of CASK-KD. We confirmed that our shRNA construct for GluN2B (shGluN2B)[46]
230 suppressed the expression of GluN2B mRNA, to 6.6% of the level of control construct-transfected
231 neurons (Supplementary Figure 9a). Introducing shGluN2B into the pyramidal neurons in layer 2/3 of
232 the somatosensory cortex by *in utero* electroporation did not affect the layer formation of the brain or
233 the migration of KD neurons (Supplementary Figure 9b). Reflecting the loss of GluN2B function, the
234 NMDA/AMPA ratio was decreased (Figure 4a, b) and the decay time constant of the NMDA current
235 was shortened in the GluN2B-KD neurons (Figure 4c, d). As observed in CASK-KD neurons, the
236 GluN2B-KD neurons had mEPSCs of increased frequency, but not amplitude (Figure 4e-g). Likewise,
237 the frequency but not the amplitude of the mIPSCs was decreased in the GluN2B-KD neurons (Figure
238 4h-j). The E/I relationship was also different between the GluN2B-KD and control neurons (Figure 4k).
239 The E/I balance index in GluN2B-KD neurons was shifted toward excitatory dominance (Figure 4l).
240 The PPR was unchanged in GluN2B-KD neurons (Supplementary Figure 10), suggesting that the
241 presynaptic release machinery was unaffected.

242

243 **GluN2B rescues the disrupted E/I balance caused by CASK deficiency.**

244 To examine whether the overexpression of GluN2B rescued CASK-KD's synaptic effects, we
245 introduced a GluN2B construct together with shCASK into the pyramidal neurons in layer 2/3 of the
246 somatosensory cortex by *in utero* electroporation, and analyzed the mPSCs. Overexpressing GluN2B in
247 the CASK-KD neurons did not affect the brain morphology (Figure 5a). Notably, the increased
248 frequency of mEPSCs and decreased frequency of mIPSCs in the CASK-KD neurons were rescued to
249 control levels by co-transfecting the GluN2B construct (Figure 5b-f). The E/I balance expressed by
250 scatter plot (Figure 5g) and the E/I balance index were also restored to the control levels (Figure 5h).

251 These results indicated that the disruption of the E/I balance caused by CASK deficiency was due to the
252 down-regulation of GluN2B function.
253
254 **Discussion**
255 In the present study, we obtained the following findings. 1) CASK was subjected to XCI in mice, in
256 which CASK-intact and -deficient neurons were distributed almost equally in a mosaic pattern in the
257 brain. 2) The frequency of mEPSCs was increased and that of mIPSCs was decreased in both
258 $CASK^{+/-}$-KO and CASK-KD neurons through a developmental mechanism. 3) These effects were not
259 rescued by overexpressing GK domain-mutant forms of CASK, which affect its interaction with TBR1.
260 4) The level of GluN2B mRNA was down-regulated in CASK-KD neurons, and overexpressing
261 GluN2B in CASK-KD neurons rescued the E/I balance impairment (Figure 5i).
262 Approximately 97% of the genes in mice and 85% of those in humans are predicted to be subject to
263 XCI[47]. We demonstrated that CASK was subjected to XCI, by single-cell genotyping combined with
264 patch-clamp electrophysiology. To our knowledge, this is the first study to use an XCI mechanism to
265 analyze molecular functions in the brain by a single-cell genotyping technique. We observed an
266 approximately 50%-50% ratio between $CASK^{+/-}$-WT and $CASK^{+/-}$-KO neurons by random sampling
267 of the pyramidal neurons in layer 2/3 of the somatosensory cortex in heterozygous CASK-KO mice
268 (Figure 1g). It is conceivable that the distribution of two different genotyped cells is skewed owing to
269 biases in the timing or microenvironment upon XCI. While we focused on a small region of the brain in
270 this study, overviewing the macroscopic distribution of CASK-deficient neurons in individual mice in
271 relation to phenotype severity may help to elucidate the pathophysiology in human cases[20, 48].
272 Atasoy et al. reported that the E/I balance is disrupted in CASK-KO cultured neurons[30]. Both
273 $CASK^{+/-}$-KO and CASK-KD replicated this effect in the pyramidal neurons in acute brain slices. This
274 effect appeared to be attributable to a developmental function of CASK, because conditional removal of

275 CASK in the adult brain did not reproduce this phenotype (Figure 2j, k). Given that differences in the
276 frequencies of mPSCs were observed between CASK$^{+/-}$-WT and CASK$^{+/-}$-KO, but not between WT
277 and CASK$^{+/-}$-WT neurons, these phenotypes were related to the postsynaptic CASK deficiency. This
278 scenario was supported by experiments performed in mosaic CASK-KD brain slices generated by *in*
279 *utero* electroporation. While the synaptic effects of CASK have been studied primarily with respect to
280 its presynaptic function[6, 7, 49, 50], our present study adds new insight that postsynaptic CASK influences
281 the E/I balance of synaptic transmission. However, we cannot exclude the possibility that presynaptic
282 CASK contributes to E/I function, and further studies are needed to clarify the presynaptic/postsynaptic
283 effects of CASK on the maintenance of E/I synapse balance. As observed in cultured neurons, the
284 membrane and firing properties in CASK$^{+/-}$-KO or CASK-KD neurons in brain slices were unchanged.
285 Thus, the seizures seen in patients with CASK mutations[19-21] are unlikely to be attributable to alterations
286 in intrinsic excitability.

287 The distorted profiles of the mPSCs in CASK-KD neurons failed to be rescued by co-transfecting
288 CASK lacking the GK domain. One well-documented function of CASK's GK domain is to mediate
289 target-gene transcription by interacting with TBR1[13-15, 43, 44]. CASK's GK domain binds to the
290 C-terminal region of TBR1, then the CASK/TBR1 complex is translocated to the nucleus, where it
291 binds the T-element of target genes to induce transcription. Thus, we speculated that the observed
292 synaptic phenotypes were mediated by a down-stream target gene of the CASK/TBR1 complex. This
293 notion was further supported by our finding that the CASK-T704A mutant failed to rescue the synaptic
294 phenotype caused by CASK deficiency (Figure 3b,e).

295 We observed a reduction in the GluN2B mRNA level in CASK-KD neurons. CASK-KO and
296 CASK-KD neurons also showed a reduced amplitude and shortened decay time constant of the NMDA
297 receptor-mediated currents, suggesting that the GluN2B function was down-regulated. GluN2B
298 expression is decreased in TBR1-knockout mice[15, 51-54]. Considering that CASK functions as a

299 co-activator of TBR1, this decrease in GluN2B appeared to result from dysfunctional
300 CASK/TBR1-mediated transcription. GluN2B-KD neurons showed an increased mEPSC frequency
301 and decreased mIPSC frequency, mimicking the CASK-deficient synaptic phenotypes. Furthermore,
302 overexpressing GluN2B restored the altered mPSCs in CASK-KD neurons.

303 The roles GluN2B in excitatory synaptic functions have been studied in GluN2B-KD and -KO
304 hippocampal neurons, both of which exhibit an increased mEPSC frequency[46, 55-57], as we observed. In
305 addition, we analyzed the effect of GluN2B deficiency on inhibitory synaptic functions and found that
306 the change was shifted in the opposite direction. Changes in the frequency, but not amplitude, of mPSCs
307 suggest that the anomaly is in the presynapses. The absence of a PPR phenotype in both excitatory and
308 inhibitory synaptic transmission indicated that the number of functional synapses projecting onto
309 CASK-deficient neurons may be altered.

310 In summary, our study provides evidence for a molecular mechanism in which CASK deficiency
311 down-regulates the GluN2B subunit of NMDA receptors, due to the loss of CASK's GK domain,
312 resulting in disruption of the E/I synaptic balance in the brain. Further studies addressing how a mosaic
313 deficiency of CASK in neural circuits causes defective brain functions are needed to understand the
314 pathophysiology of CASK-deficient diseases.

315

316

317 Supplementary information is available at the *Molecular Psychiatry* website.

318

319 **Acknowledgements**

320 We thank all of the Tabuchi lab members for helpful comments and technical support. This work was
321 supported by Grant-in-Aid for Young Scientists (B) 25871060 (T.M.), Grant-in-Aid for Scientific
322 Research (C) 17K01975 (T.M.), Grant-in-Aid for Scientific Research (B) 25290021 (T.U.) and

25282242 (K.T.), Grant-in-Aid for challenging Exploratory Research 26640039 (T.U.), 16K14592, 24650183 (K.T.), and 15K15730 (T.Y.), the Foundation of Growth Science (T.M.), the Japan Epilepsy Research Foundation (T.M.), the Takeda Science Foundation (T.U and K.T.), the Uehara Memorial Foundation (K.T.), the Ichiro Kanehara Foundation (K.T.), CREST, JST (JPMJCR1XM5, T.U.), and the JST PRESTO Program: Development and Foundation of Neural Networks (K.T.).

Competing financial interests.

The authors declare no competing financial interests.

References

1. Hsueh YP. The role of the MAGUK protein CASK in neural development and synaptic function. *Current medicinal chemistry* 2006; **13**(16): 1915-1927.

2. Won S, Levy JM, Nicoll RA, Roche KW. MAGUKs: multifaceted synaptic organizers. *Current opinion in neurobiology* 2017; **43**: 94-101.

3. Hsueh YP. Calcium/calmodulin-dependent serine protein kinase and mental retardation. *Annals of neurology* 2009; **66**(4): 438-443.

4. Hata Y, Butz S, Sudhof TC. CASK: a novel dlg/PSD95 homolog with an N-terminal calmodulin-dependent protein kinase domain identified by interaction with neurexins. *The Journal of neuroscience : the official journal of the Society for Neuroscience* 1996; **16**(8): 2488-2494.

5. Setou M, Nakagawa T, Seog DH, Hirokawa N. Kinesin superfamily motor protein KIF17 and mLin-10 in NMDA receptor-containing vesicle transport. *Science* 2000; **288**(5472): 1796-1802.

6. Tabuchi K, Biederer T, Butz S, Sudhof TC. CASK participates in alternative tripartite complexes in which Mint 1 competes for binding with caskin 1, a novel CASK-binding protein. *The Journal of neuroscience : the official journal of the Society for Neuroscience* 2002; **22**(11): 4264-4273.

7. Mukherjee K, Sharma M, Urlaub H, Bourenkov GP, Jahn R, Sudhof TC *et al.* CASK Functions as a Mg2+-independent neurexin kinase. *Cell* 2008; **133**(2): 328-339.

8. Stafford RL, Ear J, Knight MJ, Bowie JU. The molecular basis of the Caskin1 and Mint1 interaction with CASK. *Journal of molecular biology* 2011; **412**(1): 3-13.

9. LaConte LE, Chavan V, Liang C, Willis J, Schonhense EM, Schoch S *et al.* CASK stabilizes neurexin and links it to liprin-alpha in a neuronal activity-dependent manner. *Cellular and molecular life sciences : CMLS* 2016; **73**(18): 3599-3621.

367 10. Hsueh YP, Yang FC, Kharazia V, Naisbitt S, Cohen AR, Weinberg RJ *et al.* Direct
368 interaction of CASK/LIN-2 and syndecan heparan sulfate proteoglycan and their
369 overlapping distribution in neuronal synapses. *The Journal of cell biology* 1998;
370 **142**(1): 139-151.
371
372 11. Cohen AR, Woods DF, Marfatia SM, Walther Z, Chishti AH, Anderson JM.
373 Human CASK/LIN-2 binds syndecan-2 and protein 4.1 and localizes to the
374 basolateral membrane of epithelial cells. *The Journal of cell biology* 1998; **142**(1):
375 129-138.
376
377 12. Jeyifous O, Waites CL, Specht CG, Fujisawa S, Schubert M, Lin EI *et al.* SAP97
378 and CASK mediate sorting of NMDA receptors through a previously unknown
379 secretory pathway. *Nature neuroscience* 2009; **12**(8): 1011-1019.
380
381 13. Hsueh YP, Wang TF, Yang FC, Sheng M. Nuclear translocation and transcription
382 regulation by the membrane-associated guanylate kinase CASK/LIN-2. *Nature*
383 2000; **404**(6775): 298-302.
384
385 14. Wang GS, Hong CJ, Yen TY, Huang HY, Ou Y, Huang TN *et al.* Transcriptional
386 modification by a CASK-interacting nucleosome assembly protein. *Neuron* 2004;
387 **42**(1): 113-128.
388
389 15. Wang TF, Ding CN, Wang GS, Luo SC, Lin YL, Ruan Y *et al.* Identification of
390 Tbr-1/CASK complex target genes in neurons. *Journal of neurochemistry* 2004;
391 **91**(6): 1483-1492.
392
393 16. Sudhof TC. Synaptic Neurexin Complexes: A Molecular Code for the Logic of
394 Neural Circuits. *Cell* 2017; **171**(4): 745-769.
395
396 17. Tarpey PS, Smith R, Pleasance E, Whibley A, Edkins S, Hardy C *et al.* A
397 systematic, large-scale resequencing screen of X-chromosome coding exons in
398 mental retardation. *Nature genetics* 2009; **41**(5): 535-543.
399
400 18. Hackett A, Tarpey PS, Licata A, Cox J, Whibley A, Boyle J *et al.* CASK mutations
401 are frequent in males and cause X-linked nystagmus and variable XLMR
402 phenotypes. *European journal of human genetics : EJHG* 2010; **18**(5): 544-552.

19. Saitsu H, Kato M, Osaka H, Moriyama N, Horita H, Nishiyama K *et al.* CASK aberrations in male patients with Ohtahara syndrome and cerebellar hypoplasia. *Epilepsia* 2012; **53**(8): 1441-1449.

20. Nakajiri T, Kobayashi K, Okamoto N, Oka M, Miya F, Kosaki K *et al.* Late-onset epileptic spasms in a female patient with a CASK mutation. *Brain & development* 2015; **37**(9): 919-923.

21. Michaud JL, Lachance M, Hamdan FF, Carmant L, Lortie A, Diadori P *et al.* The genetic landscape of infantile spasms. *Human molecular genetics* 2014; **23**(18): 4846-4858.

22. Hayashi S, Okamoto N, Chinen Y, Takanashi J, Makita Y, Hata A *et al.* Novel intragenic duplications and mutations of CASK in patients with mental retardation and microcephaly with pontine and cerebellar hypoplasia (MICPCH). *Human genetics* 2012; **131**(1): 99-110.

23. Najm J, Horn D, Wimplinger I, Golden JA, Chizhikov VV, Sudi J *et al.* Mutations of CASK cause an X-linked brain malformation phenotype with microcephaly and hypoplasia of the brainstem and cerebellum. *Nature genetics* 2008; **40**(9): 1065-1067.

24. Piluso G, D'Amico F, Saccone V, Bismuto E, Rotundo IL, Di Domenico M *et al.* A missense mutation in CASK causes FG syndrome in an Italian family. *American journal of human genetics* 2009; **84**(2): 162-177.

25. Piluso G, Carella M, D'Avanzo M, Santinelli R, Carrano EM, D'Avanzo A *et al.* Genetic heterogeneity of FG syndrome: a fourth locus (FGS4) maps to Xp11.4-p11.3 in an Italian family. *Human genetics* 2003; **112**(2): 124-130.

26. Moog U, Kutsche K, Kortum F, Chilian B, Bierhals T, Apeshiotis N *et al.* Phenotypic spectrum associated with CASK loss-of-function mutations. *Journal of medical genetics* 2011; **48**(11): 741-751.

27. Takanashi J, Okamoto N, Yamamoto Y, Hayashi S, Arai H, Takahashi Y *et al.* Clinical and radiological features of Japanese patients with a severe phenotype due to CASK mutations. *American journal of medical genetics Part A* 2012; **158A**(12): 3112-3118.

28. Dimitratos SD, Stathakis DG, Nelson CA, Woods DF, Bryant PJ. The location of human CASK at Xp11.4 identifies this gene as a candidate for X-linked optic atrophy. *Genomics* 1998; **51**(2): 308-309.

29. Stevenson D, Laverty HG, Wenwieser S, Douglas M, Wilson JB. Mapping and expression analysis of the human CASK gene. *Mammalian genome : official journal of the International Mammalian Genome Society* 2000; **11**(10): 934-937.

30. Atasoy D, Schoch S, Ho A, Nadasy KA, Liu X, Zhang W *et al.* Deletion of CASK in mice is lethal and impairs synaptic function. *Proceedings of the National Academy of Sciences of the United States of America* 2007; **104**(7): 2525-2530.

31. Augui S, Nora EP, Heard E. Regulation of X-chromosome inactivation by the X-inactivation centre. *Nature reviews Genetics* 2011; **12**(6): 429-442.

32. Wu H, Luo J, Yu H, Rattner A, Mo A, Wang Y *et al.* Cellular resolution maps of X chromosome inactivation: implications for neural development, function, and disease. *Neuron* 2014; **81**(1): 103-119.

33. de Vries WN, Binns LT, Fancher KS, Dean J, Moore R, Kemler R *et al.* Expression of Cre recombinase in mouse oocytes: a means to study maternal effect genes. *Genesis* 2000; **26**(2): 110-112.

34. Maximov A, Tang J, Yang X, Pang ZP, Sudhof TC. Complexin controls the force transfer from SNARE complexes to membranes in fusion. *Science* 2009; **323**(5913): 516-521.

35. Uemura T, Mori T, Kurihara T, Kawase S, Koike R, Satoga M *et al.* Fluorescent protein tagging of endogenous protein in brain neurons using CRISPR/Cas9-mediated knock-in and in utero electroporation techniques. *Scientific reports* 2016; **6**: 35861.

36. Mori T, Morimoto K. Rabies virus glycoprotein variants display different patterns in rabies monosynaptic tracing. *Frontiers in neuroanatomy* 2014; **7**: 47.

37. Tabuchi K, Blundell J, Etherton MR, Hammer RE, Liu X, Powell CM *et al.* A neuroligin-3 mutation implicated in autism increases inhibitory synaptic transmission in mice. *Science* 2007; **318**(5847): 71-76.

38. Maximov A, Sudhof TC, Bezprozvanny I. Association of neuronal calcium channels with modular adaptor proteins. *The Journal of biological chemistry* 1999; **274**(35): 24453-24456.

39. Nafzger S, Rougier JS. Calcium/calmodulin-dependent serine protein kinase CASK modulates the L-type calcium current. *Cell calcium* 2017; **61**: 10-21.

40. Leonoudakis D, Conti LR, Radeke CM, McGuire LM, Vandenberg CA. A multiprotein trafficking complex composed of SAP97, CASK, Veli, and Mint1 is associated with inward rectifier Kir2 potassium channels. *The Journal of biological chemistry* 2004; **279**(18): 19051-19063.

41. Eichel CA, Beuriot A, Chevalier MY, Rougier JS, Louault F, Dilanian G *et al.* Lateral Membrane-Specific MAGUK CASK Down-Regulates NaV1.5 Channel in Cardiac Myocytes. *Circulation research* 2016; **119**(4): 544-556.

42. Monyer H, Burnashev N, Laurie DJ, Sakmann B, Seeburg PH. Developmental and regional expression in the rat brain and functional properties of four NMDA receptors. *Neuron* 1994; **12**(3): 529-540.

43. Huang TN, Chang HP, Hsueh YP. CASK phosphorylation by PKA regulates the protein-protein interactions of CASK and expression of the NMDAR2b gene. *Journal of neurochemistry* 2010; **112**(6): 1562-1573.

44. Huang TN, Hsueh YP. CASK point mutation regulates protein-protein interactions and NR2b promoter activity. *Biochemical and biophysical research communications* 2009; **382**(1): 219-222.

45. Huang TN, Hsueh YP. Calcium/calmodulin-dependent serine protein kinase (CASK), a protein implicated in mental retardation and autism-spectrum disorders, interacts with T-Brain-1 (TBR1) to control extinction of associative memory in male mice. *Journal of psychiatry & neuroscience : JPN* 2017; **42**(1): 37-47.

46. Kim MJ, Dunah AW, Wang YT, Sheng M. Differential roles of NR2A- and NR2B-containing NMDA receptors in Ras-ERK signaling and AMPA receptor trafficking. *Neuron* 2005; **46**(5): 745-760.

47. Berletch JB, Yang F, Disteche CM. Escape from X inactivation in mice and humans. *Genome biology* 2010; **11**(6): 213.

48. Srivastava S, McMillan R, Willis J, Clark H, Chavan V, Liang C *et al.* X-linked intellectual disability gene CASK regulates postnatal brain growth in a non-cell autonomous manner. *Acta neuropathologica communications* 2016; **4**: 30.

49. Maximov A, Bezprozvanny I. Synaptic targeting of N-type calcium channels in hippocampal neurons. *The Journal of neuroscience : the official journal of the Society for Neuroscience* 2002; **22**(16): 6939-6952.

50. Biederer T, Sudhof TC. CASK and protein 4.1 support F-actin nucleation on neurexins. *The Journal of biological chemistry* 2001; **276**(51): 47869-47876.

51. Huang TN, Hsueh YP. Brain-specific transcriptional regulator T-brain-1 controls brain wiring and neuronal activity in autism spectrum disorders. *Frontiers in neuroscience* 2015; **9**: 406.

52. Chuang HC, Huang TN, Hsueh YP. T-Brain-1--A Potential Master Regulator in Autism Spectrum Disorders. *Autism research : official journal of the International Society for Autism Research* 2015; **8**(4): 412-426.

53. Huang TN, Chuang HC, Chou WH, Chen CY, Wang HF, Chou SJ *et al.* Tbr1 haploinsufficiency impairs amygdalar axonal projections and results in cognitive abnormality. *Nature neuroscience* 2014; **17**(2): 240-247.

54. Chuang HC, Huang TN, Hsueh YP. Neuronal excitation upregulates Tbr1, a high-confidence risk gene of autism, mediating Grin2b expression in the adult brain. *Frontiers in cellular neuroscience* 2014; **8**: 280.

55. Hall BJ, Ripley B, Ghosh A. NR2B signaling regulates the development of synaptic AMPA receptor current. *The Journal of neuroscience : the official journal of the Society for Neuroscience* 2007; **27**(49): 13446-13456.

56. Wang CC, Held RG, Chang SC, Yang L, Delpire E, Ghosh A *et al.* A critical role for GluN2B-containing NMDA receptors in cortical development and function. *Neuron* 2011; **72**(5): 789-805.

57. Gray JA, Shi Y, Usui H, During MJ, Sakimura K, Nicoll RA. Distinct modes of AMPA receptor suppression at developing synapses by GluN2A and GluN2B: single-cell NMDA receptor subunit deletion in vivo. *Neuron* 2011; **71**(6): 1085-1101.

565 **Figure Legends**

566 **Figure 1. CASK is subjected to XCI in female mice.**

567 a. Survival rate of CASK KO and WT mice. ~25% of the $CASK^{+/-}$ mice died within 15 days.
568 Percentage of live animals of each genotype is shown. $CASK^{+/+}$ (black, $n = 12$), $CASK^{Y/+}$ (gray, $n = 10$),
569 $CASK^{+/-}$ (red, $n = 14$), and $CASK^{Y/-}$ (green, $n = 10$).

570 b. Photographs of $CASK^{+/+}$ (left) and $CASK^{+/-}$ (right) female mice at 7 days of age. The $CASK^{+/-}$ mice
571 were smaller than the $CASK^{+/+}$ mice. Scale bar represents 1 cm.

572 c. Growth curve of CASK KO and WT mice. $CASK^{+/-}$ mice ($n = 10$) were smaller than $CASK^{+/+}$ ($n =$
573 10) and $CASK^{Y/+}$ ($n = 12$) mice.

574 d. DAPI staining of the somatosensory cortex of 5-week-old $CASK^{+/+}$ (left) and $CASK^{+/-}$ (right) mice.
575 Numbers indicate cortical layers. Scale bar: 100 μm.

576 e. Schematic illustration of XCI and single-cell genotyping in heterozygous CASK KO mice. In the
577 progenitor cells of female heterozygous CASK KO mice, one of the X chromosomes is randomly
578 selected and inactivated by XCI early in development. The XCI pattern is transferred to their daughter
579 cells during cell division, resulting in a mosaic distribution pattern of the CASK WT and CASK KO
580 cells in tissues. In adult brain slices, the genotypes and physiological functions of neurons were
581 examined by patch-clamp recording followed by single-cell RT-PCR.

582 f. Agarose gel electrophoresis image of single-cell RT-PCR. Positions of the primer sets for the RT-PCR
583 of CASK are shown above. Note that the CASK band is absent in the right-most lane (KO; CASK-). M,
584 100-bp DNA ladder; Act, β-actin PCR product; Cask, CASK PCR product.

585 g. Percentage of CASK-positive cells. CASK expression was detected in about half of the cells in the
586 $CASK^{+/-}$ brains. $CASK^{+/+}$, $n = 6$ animals; and $CASK^{+/-}$, $n = 10$ animals. Numbers on bars are the
587 CASK-positive cells/total cells analyzed.

588 h. Representative traces of the membrane potential of CASK-positive (WT, left, blue traces) and
589 -negative (KO, right, red traces) neurons from a $CASK^{+/-}$ mouse. The CASK genotypes of the recorded
590 neurons of $CASK^{+/-}$ mice were determined by single-cell RT-PCR. Scale bars represent 20 mV (vertical
591 axis) and 0.2 s (horizontal axis). 0 mV indicates the potential at the ground.
592 i-n. Resting membrane potential (i), AP threshold (j), AP amplitude (k), AP half-time width (l), input
593 resistance (m), and input (injected current)/output (spike number) curve (n) of WT ($CASK^{+/+}$, $CASK^{Y/+}$,
594 $CASK^{+/-}$ WT) and $CASK^{+/-}$ KO neurons. (Animal numbers; $CASK^{+/+}$ female n=3, $CASK^{Y/+}$ male n=3,
595 $CASK^{+/-}$ female n=7).
596 Numbers on bars are the numbers of cells analyzed (i-m). * $p < 0.05$, ** $p < 0.01$, as examined by
597 ANOVA and Bonferroni's post-hoc test.
598
599 **Figure 2. CASK deficiency disrupts the E/I balance and NMDA receptor-mediated synaptic**
600 **function in a developmental mechanism.**
601 a. Representative traces of miniature excitatory postsynaptic currents (mEPSCs) in neurons with four
602 different genotypes. The CASK genotype of the recorded neurons from $CASK^{+/-}$ mice was determined
603 by single-cell RT-PCR. Scale bars represent 10 pA (vertical axis) and 1 s (horizontal axis).
604 b-c. Frequency (b) and amplitude (c) of the mEPSCs in neurons with four different genotypes. The
605 frequency of mEPSCs in CASK-deficient neurons ($CASK^{+/-}$-KO) was increased. Numbers on bars
606 represent the number of cells recorded. (Animal numbers; $CASK^{+/+}$ female n=3, $CASK^{Y/+}$ male n=3,
607 $CASK^{+/-}$ female n=7)
608 d. Representative traces of the mIPSCs in neurons with four different genotypes. The CASK genotype
609 of the recorded neurons from $CASK^{+/-}$ mice was determined by single-cell RT-PCR. Scale bars
610 represent 10 pA (vertical axis) and 1 s (horizontal axis).

611 e-f. Frequency (e) and amplitude (f) of the mIPSCs in neurons with four different genotypes. The
612 frequency of the mIPSCs in CASK-deficient neurons ($CASK^{+/-}$-KO) was decreased. Numbers on bars
613 represent the number of cells recorded. (Animal numbers; $CASK^{+/+}$ female n=3, $CASK^{Y/+}$ male n=3,
614 $CASK^{+/-}$ female n=7)
615 g. Scatter plot of the frequency of mEPSCs versus mIPSCs in neurons with four different genotypes.
616 Each dot represents a single cell. CASK-deficient cells ($CASK^{+/-}$-KO) showed a different pattern from
617 those of the other genotypes.
618 h. E/I balance index for each genotype. The E/I balance of CASK-deficient cells ($CASK^{+/-}$-KO) was
619 shifted toward excitatory dominance. Numbers on bars represent the number of cells recorded.
620 i. AAV-Cre-mediated conditional knockout of CASK. The timings of AAV injection and recording (top),
621 a histological image of the AAV-injected area (middle), and a schematic illustration of the conditional
622 deletion of CASK in a cell and confocal images for CASK immunostaning (red) in AAV-CreGFP
623 (green) infected brains in wild-type and CASK-floxed mice (bottom) are shown. Note that the CASK
624 and GFP double positive neurons are missing in CASK-floxed mice. Scale bars are 100 (middle) and 50
625 (bottom) μm.
626 j and k. Frequency and amplitude of mEPSCs (l) and mIPSCs (m) were unaltered in CASK conditional
627 KO neurons (green). Numbers on bars represent the number of cells recorded. (Animal numbers; floxed
628 CASK+GFPCre n=4, floxed CASK+GFP n=3, floxed CASK n=3, WT+GFPCre n=3)
629 l. Paired-pulse ratios of evoked excitatory and inhibitory postsynaptic contents (ePPR and iPPR) were
630 unaltered in $CASK^{+/-}$-KO neurons. Representative traces (left) and summary graphs (right) are shown.
631 Scale bars represent 100 pA (vertical axis) and 200 ms (horizontal axis). Numbers on bars represent the
632 number of cells recorded. (Animal numbers; $CASK^{+/-}$ female n=9)
633 m. Representative traces (left) and summary graphs (right) of the NMDA/AMPA ratio and NMDA
634 decay time constant of WT and $CASK^{+/-}$-KO neurons. The NMDA/AMPA ratio and decay time

635 constant of the NMDA current were decreased in CASK$^{+/-}$-KO neurons. Scale bar represents 200 ms.
636 Numbers on bars represent the number of cells recorded. (Animal numbers; CASK$^{+/-}$ female n=8)
637 Statistical significance was determined by ANOVA and Bonferroni's post-hoc test. * $p < 0.05$, *** $p <$
638 0.001.
639
640 **Figure 3. The guanylate kinase domain of CASK is responsible for the disrupted E/I balance and**
641 **NMDA receptor function in CASK KD neurons.**
642 a-h. Miniature postsynaptic currents of control and CASK-KD neurons co-transfected with or without
643 various rescue constructs in layer 2/3 of the somatosensory cortex. Representative traces (a) and graphs
644 of the frequency (b) and amplitude (c) of mEPSCs. Representative traces (d), summary graphs of the
645 frequency (e) and amplitude (f) of mIPSCs. FL, full-length; ΔC, CAM domain deleted; ΔL, LIN
646 domain deleted; ΔP, PDZ domain deleted; ΔS, SH3 domain deleted; ΔG and ΔGK, GK domain deleted;
647 TA, T704A mutant of CASK. The CASK ΔG or TA constructs failed to rescue the increased frequency
648 of mEPSCs (b) or the decreased frequency of mIPSCs (e) in CASK KD neurons. Scale bars represent
649 10 pA (vertical axis) (a) and 20 pA (vertical axis) (d) and 1 s (horizontal axis) (a and d). (Animal
650 numbers; n=3 in each condition)
651 g. Distribution of the frequency of mEPSCs versus mIPSCs for neurons of four genotypes. Each dot
652 represents a single cell.
653 h. E/I balance index for neurons with each KD.
654 i. Representative traces of evoked AMPA (lower trace) and NMDA (upper trace) receptor-medicated
655 synaptic currents in control and CASK-KD neurons. Scale bars represent 50 pA (vertical axis) and 0.2 s
656 (horizontal axis).
657 j. Graph of the NMDA/AMPA ratio in control, CASK-KD, and CASK-KD + rescue vector transfected
658 neurons. (Animal numbers; n=3 in each condition)

659 k. Normalized traces of NMDA receptor-mediated currents recorded from control and CASK-KD
660 neurons were superimposed. Scale bar represents 0.2 s.
661 l. Weighted decay time constant (τ) of the NMDA receptor-mediated current in control, CASK-KD, and
662 CASK-KD + rescue vector transfected neurons. The decay time constant of the NMDA current was
663 decreased in CASK-KD neurons, and was not rescued by CASKΔGK co-transfection.
664 m. The mRNA (left) and protein (middle) levels of GluN2A and GluN2B in control and CASK-KD
665 neurons examined by qRT-PCR and immunoblot, respectively. Representative images (right) of
666 immunoblot bands of β-actin, GluN2A and GluN2B obtained from control and CASK-KD neurons.
667 (Sample numbers; Cntl n=3, shCASK n=3 in mRNA. Cntl n=5, shCASK n=5 in protein)
668 Statistical significance was determined by unpaired t-test (m) or by ANOVA and Bonferroni's post-hoc
669 test (b, c, e, f, h, j and l). * $p < 0.05$, ** $p < 0.01$, *** $p < 0.001$. Numbers on bars are the number of cells
670 analyzed.
671
672 **Figure 4. GluN2B-KD disrupts the E/I balance in pyramidal neurons in layer 2/3 of the**
673 **somatosensory cortex.**
674 a. Representative traces of evoked AMPA (lower trace) and NMDA (upper trace) receptor-mediated
675 synaptic currents in control (black) and shGluN2B-transfected (green) neurons. Scale bars represent 50
676 pA (vertical axis) and 0.2 s (horizontal axis).
677 b. NMDA/AMPA ratio in control and shGluN2B-transfected neurons. The NMDA/AMPA ratio was
678 significantly decreased in the shGluN2B-transfected neurons. (Animal numbers; Cntl n=3, shGluN2B
679 n=3)
680 c. Normalized sample traces of NMDA receptor-mediated synaptic currents recorded from control and
681 shGluN2B-transfected neurons. Fitted double exponential curves are shown in red. Scale bar represents
682 0.2 s.

683 d. Weighted decay time constant (τ) of the NMDA receptor-mediated current in control and
684 shGluN2B-transfected neurons. The decay time constant (τ) in shGluN2B-transfected neurons was
685 decreased compared to control neurons. (Animal numbers; Cntl n=3, shGluN2B n=3)
686 e. Representative traces of the mEPSC in control (upper) and shGluN2B-transfected (lower) neurons.
687 Scale bars represent 10 pA (vertical axis) and 1 s (horizontal axis).
688 f-g. Frequency (f) and amplitude (g) of the mEPSC in control and shGluN2B-transfected neurons. The
689 frequency of the mEPSC was increased by GluN2B-KD. (Animal numbers; Cntl n=3, shGluN2B n=3)
690 h. Representative traces of the mIPSC in control (upper) and shGluN2B-transfected (lower) neurons.
691 Scale bars represent 10 pA (vertical axis) and 1 s (horizontal axis).
692 i-j. Frequency (i) and amplitude (j) of the mIPSC in control and shGluN2B-transfected neurons. The
693 frequency of the mIPSC was decreased by GluN2B-KD. (Animal numbers; Cntl n=3, shGluN2B n=3)
694 k. Scatter plot of the frequency of mEPSCs versus mIPSCs in control and shGluN2B-transfected
695 neurons. Each dot represents a single cell. The control and shGluN2B-transfected neurons showed
696 different distributions.
697 l. E/I balance index of control and shGluN2B-transfected neurons.
698 Statistical significance was determined by unpaired *t*-test. * $p < 0.05$, *** $p < 0.001$. Numbers on bars
699 are the number of cells analyzed.
700
701 **Figure 5. Co-transfection with GluN2B rescues the disrupted E/I balance in the spontaneous**
702 **synaptic transmission in CASK KD neurons.**
703 a. Histological images of shCASK + GluN2B-transfected somatosensory cortex. The laminar structure
704 was visualized by DAPI staining (left). tdTomato-labeled shCASK + GluN2B-transfected neurons were
705 in layer 2/3 of the somatosensory cortex (right). Cortical layers are indicated by numbers. Scale bar: 100
706 μm.

b. Representative traces of the mEPSC (left) and mIPSC (right) from shCASK neurons (top) and shCASK + GluN2B neurons (bottom). Scale bars represent 10 pA (vertical axis) and 1 s (horizontal axis).

c-d. Frequency (c) and amplitude (d) of the mEPSC in control (black), shCASK (red), and shCASK + GluN2B (green) neurons. GluN2B transfection rescued the increased mEPSC frequency in shCASK-transfected neurons. (Animal numbers; Cntl n=3, shCASK n=3, shCASK+GluN2B n=3)

e-f. Frequency (e) and amplitude (f) of the mIPSCs in control, shCASK, and shCASK + GluN2B neurons. GluN2B transfection rescued the decreased mIPSC frequency in the shCASK-transfected neurons.

g. Distribution of the frequency of mEPSCs versus mIPSCs shown in a scatter plot. Each dot represents a single cell.

h. E/I balance index of neurons with each KD.

i. Molecular mechanism underlying the disruption of the E/I synaptic balance in CASK heterozygous female mice. Either the CASK KO or WT allele is randomly inhibited (Xi) by XCI, and the activated X chromosome (Xa) determines the genotype of the cell. In CASK KO neurons, GluN2B expression is down-regulated, resulting in a shifting of the E/I synaptic balance toward excitatory dominance.

Statistical significance was determined by ANOVA and Bonferroni's post-hoc test (c–f, and h). * $p < 0.05$, ** $p < 0.01$, *** $p < 0.001$. Numbers on bars are the number of cells analyzed.

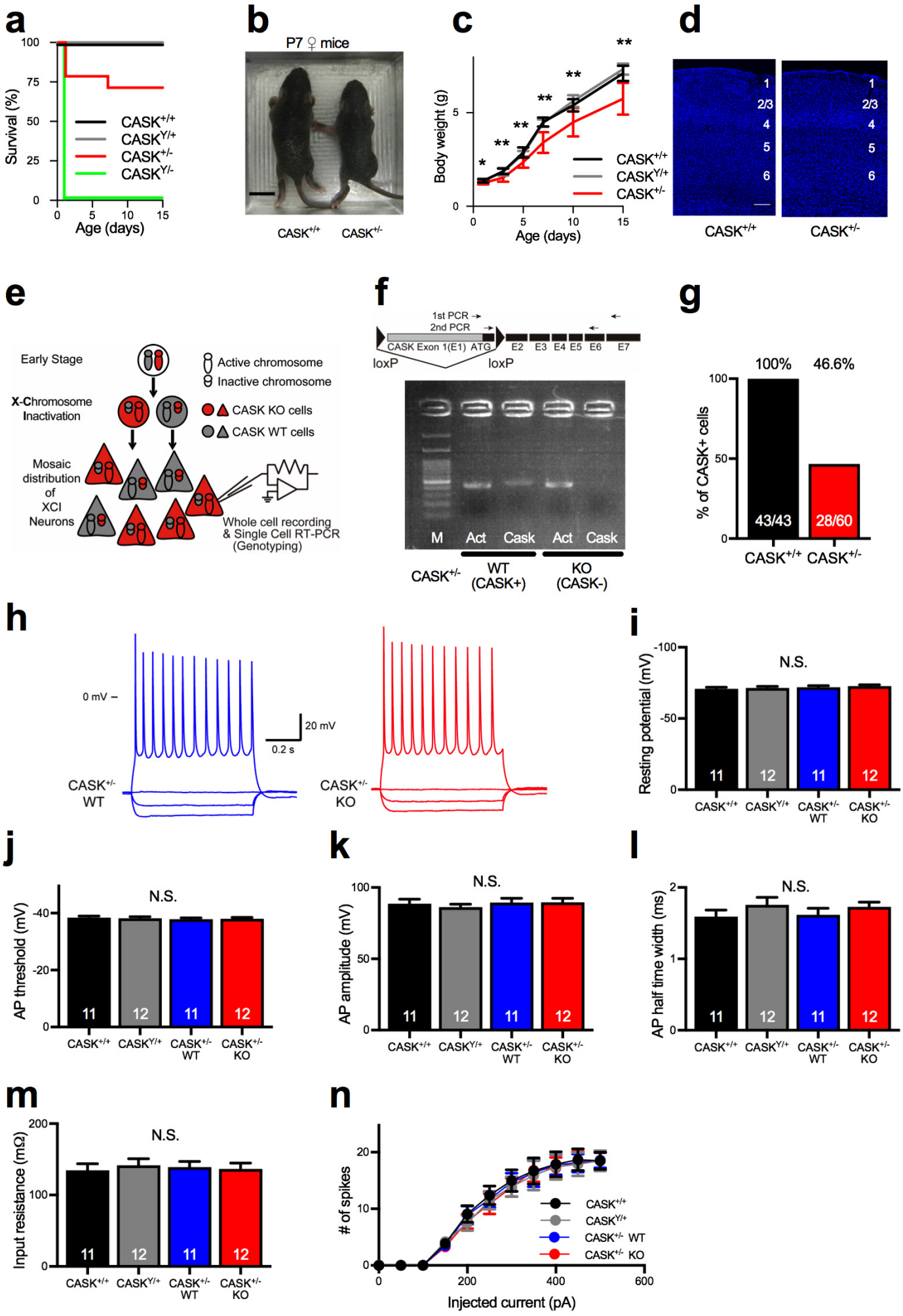
a
Survival (%)
Age (days)
CASK+/+
CASKY/+
CASK+/-
CASKY/-
b
P7 ♀ mice
CASK+/+
CASK+/-
c
Body weight (g)
Age (days)
CASK+/+
CASKY/+
CASK+/-
d
1
2/3
4
5
6
CASK+/+
CASK+/-
e
Early Stage
X-Chromosome Inactivation
Mosaic distribution of XCI Neurons
Active chromosome
Inactive chromosome
CASK KO cells
CASK WT cells
Whole cell recording & Single Cell RT-PCR (Genotyping)
f
1st PCR
2nd PCR
CASK Exon 1(E1) ATG
E2 E3 E4 E5 E6 E7
loxP
loxP
M
Act
Cask
Act
Cask
CASK+/-
WT (CASK+)
KO (CASK-)
g
100%
46.6%
% of CASK+ cells
43/43
28/60
CASK+/+
CASK+/-
h
0 mV
20 mV
0.2 s
CASK+/- WT
CASK+/- KO
i
Resting potential (mV)
N.S.
11
12
11
12
CASK+/+
CASKY/+
CASK+/- WT
CASK+/- KO
j
AP threshold (mV)
N.S.
11
12
11
12
CASK+/+
CASKY/+
CASK+/- WT
CASK+/- KO
k
AP amplitude (mV)
N.S.
11
12
11
12
CASK+/+
CASKY/+
CASK+/- WT
CASK+/- KO
l
AP half time width (ms)
N.S.
11
12
11
12
CASK+/+
CASKY/+
CASK+/- WT
CASK+/- KO
m
Input resistance (mΩ)
N.S.
11
12
11
12
CASK+/+
CASKY/+
CASK+/- WT
CASK+/- KO
n
# of spikes
Injected current (pA)
CASK+/+
CASKY/+
CASK+/- WT
CASK+/- KO

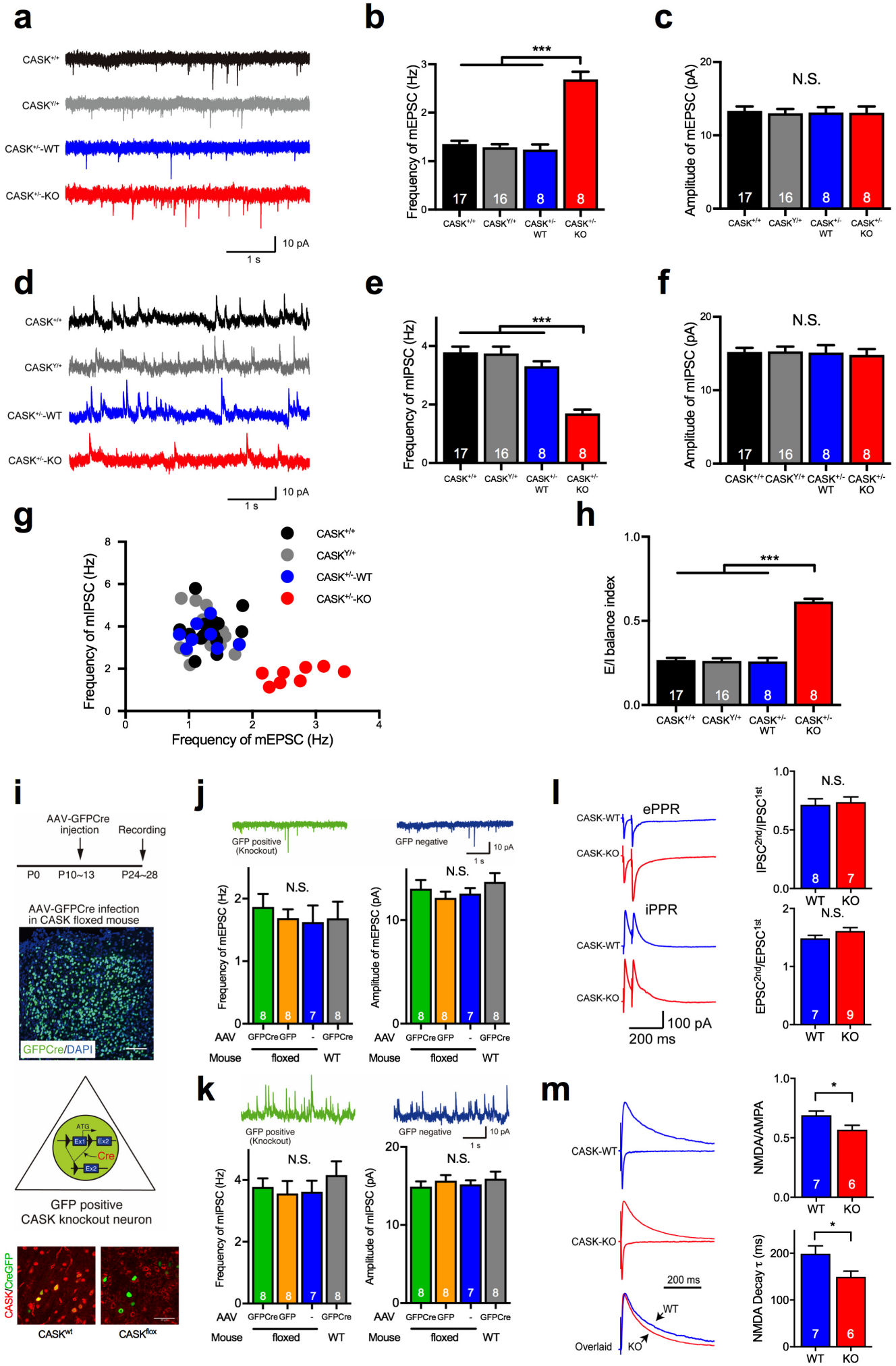
a
CASK+/+
CASKY/+
CASK+/--WT
CASK+/--KO
10 pA
1 s
b
Frequency of mEPSC (Hz)
***
17
16
8
8
CASK+/+
CASKY/+
CASK+/- WT
CASK+/- KO
c
Amplitude of mEPSC (pA)
N.S.
d
e
Frequency of mIPSC (Hz)
f
Amplitude of mIPSC (pA)
g
Frequency of mIPSC (Hz)
Frequency of mEPSC (Hz)
h
E/I balance index
i
AAV-GFPCre injection
Recording
P0
P10~13
P24~28
AAV-GFPCre infection in CASK floxed mouse
GFPCre/DAPI
GFP positive CASK knockout neuron
CASK/CreGFP
CASKwt
CASKflox
j
GFP positive (Knockout)
GFP negative
Frequency of mEPSC (Hz)
Amplitude of mEPSC (pA)
AAV
GFPCre GFP - GFPCre
Mouse
floxed
WT
k
Frequency of mIPSC (Hz)
Amplitude of mIPSC (pA)
l
ePPR
iPPR
CASK-WT
CASK-KO
100 pA
200 ms
IPSC2nd/IPSC1st
EPSC2nd/EPSC1st
m
NMDA/AMPA
NMDA Decay τ (ms)
Overlaid

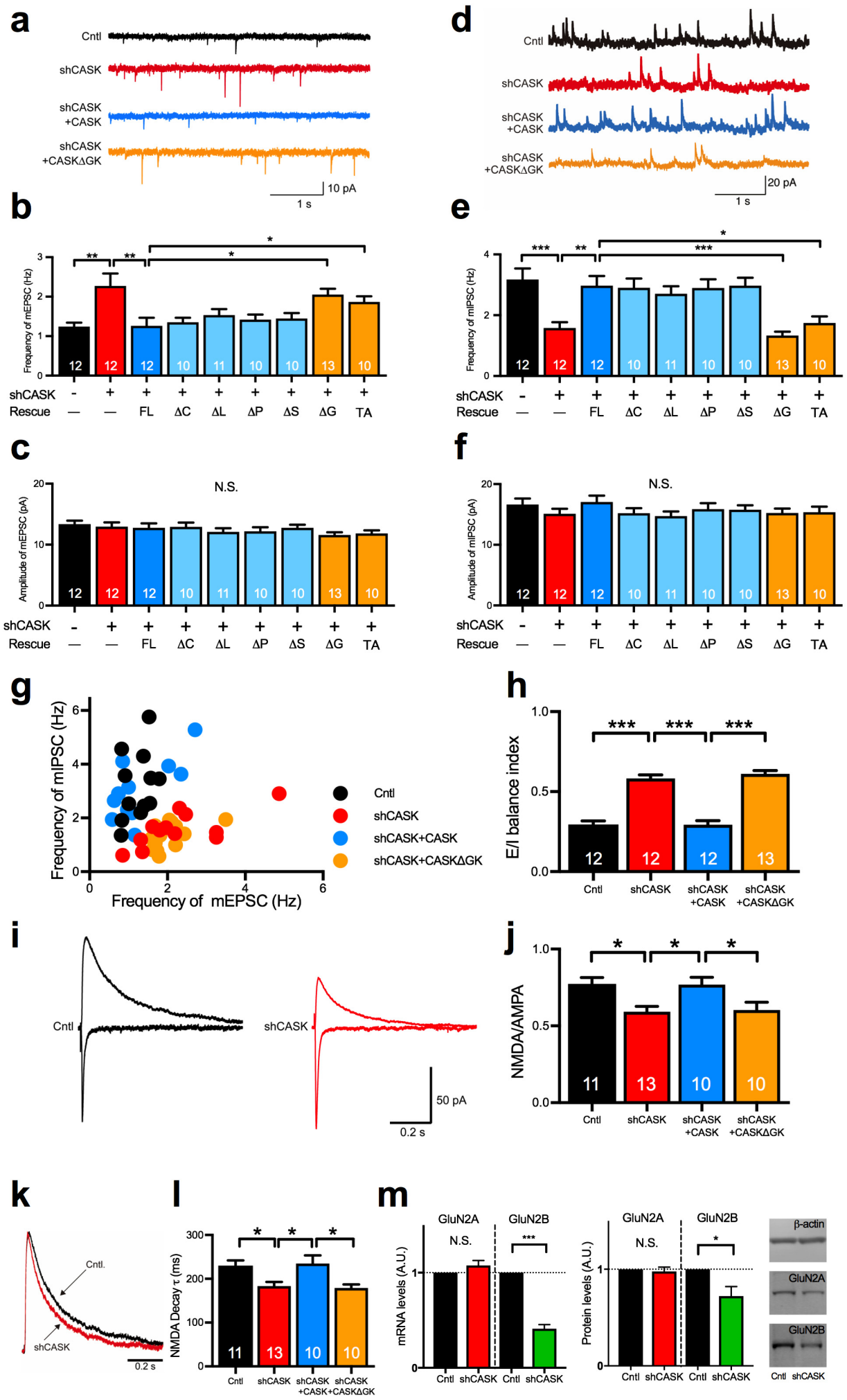
a
Cntl
shCASK
shCASK +CASK
shCASK +CASKΔGK
10 pA
1 s
d
Cntl
shCASK
shCASK +CASK
shCASK +CASKΔGK
20 pA
1 s
b
Frequency of mEPSC (Hz)
shCASK
Rescue
FL
ΔC
ΔL
ΔP
ΔS
ΔG
TA
e
Frequency of mIPSC (Hz)
c
N.S.
Amplitude of mEPSC (pA)
f
N.S.
Amplitude of mIPSC (pA)
g
Frequency of mIPSC (Hz)
Frequency of mEPSC (Hz)
Cntl
shCASK
shCASK+CASK
shCASK+CASKΔGK
h
E/I balance index
Cntl
shCASK
shCASK +CASK
shCASK +CASKΔGK
i
Cntl
shCASK
50 pA
0.2 s
j
NMDA/AMPA
k
Cntl.
shCASK
0.2 s
l
NMDA Decay τ (ms)
m
GluN2A
GluN2B
N.S.
mRNA levels (A.U.)
Protein levels (A.U.)
β-actin

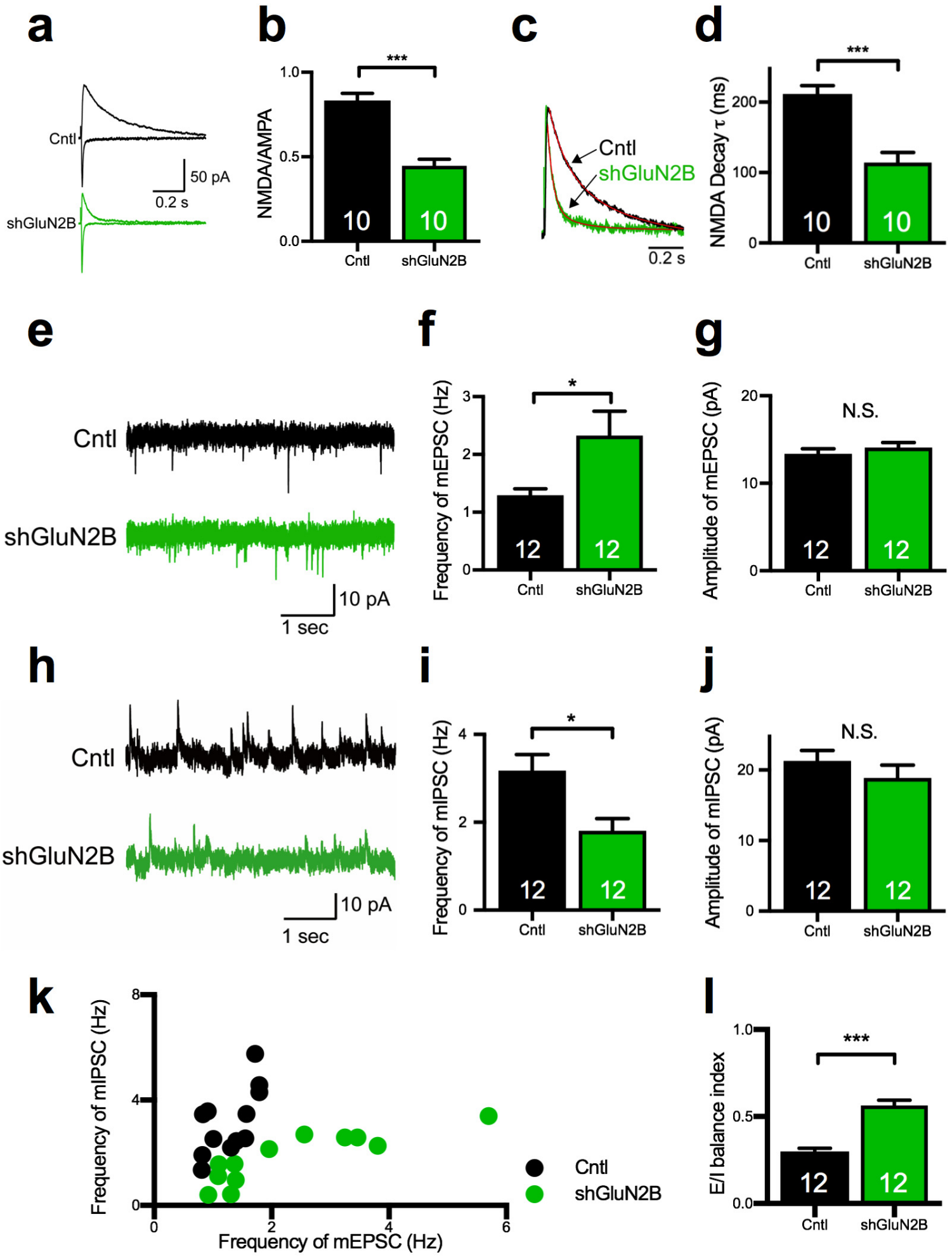
a
Cntl
shGluN2B
50 pA
0.2 s
b
***
NMDA/AMPA
1.0
0.5
0.0
10
10
Cntl
shGluN2B
c
Cntl
shGluN2B
0.2 s
d
***
NMDA Decay τ (ms)
200
100
0
10
10
Cntl
shGluN2B
e
Cntl
shGluN2B
10 pA
1 sec
f
*
Frequency of mEPSC (Hz)
3
2
1
0
12
12
Cntl
shGluN2B
g
N.S.
Amplitude of mEPSC (pA)
20
10
0
12
12
Cntl
shGluN2B
h
Cntl
shGluN2B
10 pA
1 sec
i
*
Frequency of mIPSC (Hz)
4
2
0
12
12
Cntl
shGluN2B
j
N.S.
Amplitude of mIPSC (pA)
20
10
0
12
12
Cntl
shGluN2B
k
Frequency of mIPSC (Hz)
8
4
0
0
2
4
6
Frequency of mEPSC (Hz)
Cntl
shGluN2B
l
***
E/I balance index
1.0
0.5
0.0
12
12
Cntl
shGluN2B

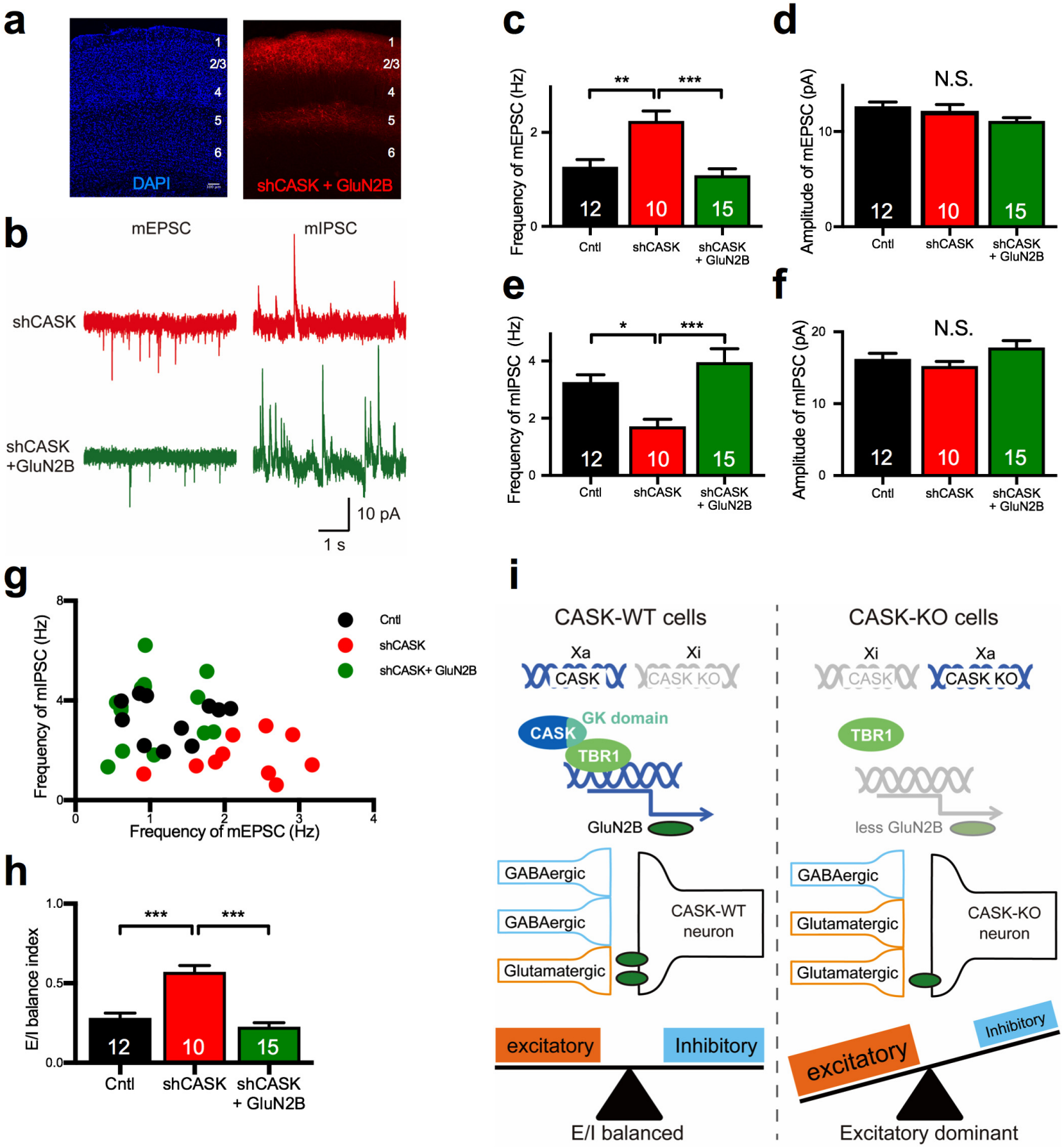
a
1
2/3
4
5
6
DAPI
shCASK + GluN2B
b
mEPSC
mIPSC
shCASK
shCASK
+GluN2B
10 pA
1 s
c
Frequency of mEPSC (Hz)
**
***
12
10
15
Cntl
shCASK
shCASK
+ GluN2B
d
Amplitude of mEPSC (pA)
N.S.
e
Frequency of mIPSC (Hz)
*
f
Amplitude of mIPSC (pA)
g
Frequency of mIPSC (Hz)
Frequency of mEPSC (Hz)
Cntl
shCASK
shCASK+ GluN2B
h
E/I balance index
i
CASK-WT cells
CASK-KO cells
Xa
Xi
CASK
CASK KO
GK domain
TBR1
GluN2B
less GluN2B
GABAergic
Glutamatergic
CASK-WT
neuron
CASK-KO
neuron
excitatory
Inhibitory
E/I balanced
Excitatory dominant